

Published in final edited form as:

Nat Clim Chang. 2015 January 1; 5(January): 41–45. doi:10.1038/nclimate2451.

A large ozone-circulation feedback and its implications for global warming assessments

Peer J. Nowack¹, N. Luke Abraham^{2,1}, Amanda C. Maycock^{1,2}, Peter Braesicke^{2,1,3}, Jonathan M. Gregory^{2,4,6}, Manoj M. Joshi^{2,4,5}, Annette Osprey^{2,4}, and John A. Pyle^{1,2}

¹Centre for Atmospheric Science, Department of Chemistry, University of Cambridge, Cambridge, United Kingdom

²National Centre for Atmospheric Science, United Kingdom

⁴Department of Meteorology, University of Reading, Reading, United Kingdom

⁶Met Office Hadley Centre, Met Office, Exeter, United Kingdom

Abstract

State-of-the-art climate models now include more climate processes which are simulated at higher spatial resolution than ever¹. Nevertheless, some processes, such as atmospheric chemical feedbacks, are still computationally expensive and are often ignored in climate simulations^{1,2}. Here we present evidence that how stratospheric ozone is represented in climate models can have a first order impact on estimates of effective climate sensitivity. Using a comprehensive atmosphere-ocean chemistry-climate model, we find an increase in global mean surface warming of around 1°C (~20%) after 75 years when ozone is prescribed at pre-industrial levels compared with when it is allowed to evolve self-consistently in response to an abrupt 4×CO₂ forcing. The difference is primarily attributed to changes in longwave radiative feedbacks associated with circulation-driven decreases in tropical lower stratospheric ozone and related stratospheric water vapour and cirrus cloud changes. This has important implications for global model intercomparison studies^{1,2} in which participating models often use simplified treatments of atmospheric composition changes that are neither consistent with the specified greenhouse gas forcing scenario nor with the associated atmospheric circulation feedbacks³⁻⁵.

Starting from pre-industrial conditions, an instantaneous quadrupling of the atmospheric CO₂ mixing ratio is a standard climate change experiment (referred to as abrupt4×CO₂) in model intercomparison projects such as the Coupled Model Intercomparison Project phase 5

Users may view, print, copy, and download text and data-mine the content in such documents, for the purposes of academic research, subject always to the full Conditions of use:http://www.nature.com/authors/editorial_policies/license.html#terms

Correspondence to: Peer J. Nowack.

³now at: Karlsruhe Institute of Technology, IMK-ASF, Karlsruhe, Germany

⁵now at: Centre for Ocean and Atmospheric Sciences, University of East Anglia, Norwich, United Kingdom

Author contributions: P.J.N. conducted the research on a day-to-day basis; the model was developed by N.L.A., J.M.G., M.M.J. and A.O.; N.L.A. and P.B. designed the initial experiment and its subsequent evolution; major analysis and interpretation of results was performed by P.J.N. and A.C.M.; P.J.N. led the paper writing, supported by A.C.M.; N.L.A., P.B. and J.A.P. all contributed to the discussion and interpretation of results and write-up; J.A.P. suggested the study.

Reprints and permissions information is available online at www.nature.com/reprints.

Competing financial interests: The authors declare no competing financial interests.

(CMIP5)¹ or the Geoenengineering Model Intercomparison Project (GeoMIP)². One aim of these initiatives is to offer a quantitative assessment of possible future climate change, with the range of projections from participating models commonly used as a measure of uncertainty⁶. Within such projects, stratospheric chemistry, and therefore stratospheric ozone, is treated differently in individual models. In CMIP5 and GeoMIP, the majority of participating models did not explicitly calculate stratospheric ozone changes^{2,4}. For abrupt4×CO₂ experiments, modelling centres thus often prescribed stratospheric ozone at pre-industrial levels^{2,5}. For transient CMIP5 experiments, it was instead recommended to use an ozone field derived from the averaged projections of 13 chemistry-climate models (CCMs)³. This multi-model mean ozone dataset was obtained from CCMVal-2 projections run under the SRES A1b scenario for well-mixed greenhouse gases, in contrast to the representative concentration pathway (RCP) scenarios used in CMIP5. To date, research on the impacts of contrasting representations of stratospheric ozone has focused on regional effects, such as the influence of possible future Antarctic ozone recovery on the position of the Southern Hemisphere mid-latitude jet^{4,7}. However, its potential effect on the magnitude of projected global warming has not received much attention.

Here, we present evidence which highlights that stratospheric chemistry-climate feedbacks can exert a more significant influence on global warming projections than has been suggested⁸. For a specific climate change experiment, we show that the choice of how to represent key stratospheric chemical species alone can result in a 20% difference in simulated global mean surface warming. Therefore, a treatment of ozone that is not internally consistent with a particular model or greenhouse gas scenario, as is the case for some CMIP5 simulations, could introduce a significant bias into climate change projections.

The model used here is a HadGEM3-AO configuration of the UK Met Office's Unified Model⁹ coupled to the UKCA stratospheric chemistry scheme¹⁰ (see Methods). This comprehensive model set-up allows us to study complex feedback effects between the atmosphere, land surface, ocean and sea-ice.

Fig. 1 shows the evolution of global and annual mean surface temperature anomalies (T_{surf}) from eight different climate integrations, two of which were carried out with interactive stratospheric chemistry and six with different prescribed monthly-mean fields of the following chemically and radiatively active gases: ozone, methane and nitrous oxide (see Table 1 for details). Experiments with label A are pre-industrial control runs. Experiment B is an abrupt4×CO₂ run with fully interactive chemistry, and experiments labelled C are non-interactive abrupt4×CO₂ runs in which the chemical fields were prescribed at pre-industrial levels. We conducted two versions of each non-interactive experiment to test the effect of using zonal mean fields (label 2, e.g. A2) instead of full 3D fields (label 1, e.g. A1). The time development of T_{surf} shows a clear difference of nearly 20% between the abrupt4×CO₂ experiments B and C1/C2, indicating a much larger global warming in C1/C2 as a consequence of missing composition feedbacks. The primary driver of these differences is changing ozone, with methane and nitrous oxide making much smaller contributions, see below. Fields averaged over the final 50 years of the interactive experiment B were imposed from the beginning in the abrupt4×CO₂ experiments B1 and B2. These simulations show a close agreement with experiment B in terms of T_{surf} , implying that the global mean energy

budget can be comparatively well-reproduced with this treatment of composition changes, despite the neglect of transient changes in their abundances.

We apply the linear regression methodology for diagnosing climate forcing and feedbacks established by Gregory *et al.*¹¹ (see also Methods) to investigate the sources of the differences between the abrupt4×CO₂ experiments with and without the effects of interactive chemistry included. The method assumes a linear relationship between the change in global and annual mean radiative imbalance at the top of the atmosphere (TOA) and T_{surf} . It has been shown to capture well the response of models to many types of climate forcing^{11,12}. The slope obtained from the regression is defined as the climate feedback parameter, α (Wm⁻²°C⁻¹). It represents a characteristic quantity of a given model system, since its magnitude approximates the T_{surf} response to a radiative forcing introduced to the system. Fig. 2a shows the Gregory regression plot for each of the 75 years after the initial abrupt 4×CO₂ forcing is imposed. The slopes diagnosed for the chemically-similar experiments B, B1 and B2 differ only slightly, however, in C1 and C2, which use the pre-industrial ozone climatologies, there is a significant decrease in the magnitude of α by ~20%, consistent with the larger T_{surf} response. The prescribed chemical fields drive the difference between experiments B1/B2 and C1/C2, so that the fundamental difference in how the modelled climate system responds to the CO₂ forcing must be connected to the changes in atmospheric composition and related further feedbacks.

To further investigate the differences, we decompose the TOA radiative fluxes into clear-sky (CS) and cloud radiative effect (CRE) components. In addition, we separate them further into shortwave (SW) and longwave (LW) contributions, producing four components in total (see Methods)¹². Fig. 2b and 2c show Gregory regressions for the two components found to be responsible for the majority of the difference in α , namely the CS-LW ($\alpha_{\text{cs,lw}}$) and the CRE-LW ($\alpha_{\text{cre,lw}}$) components (see Supplementary Fig. S1 for the smaller changes in the SW components). The differences in $\alpha_{\text{cs,lw}}$ between B and C1/C2 are of the same sign as those for α , but larger in magnitude, whereas the change in $\alpha_{\text{cre,lw}}$ is of the opposite sign and smaller in magnitude.

The reasons for the changes in the CS-LW contribution to α can be understood from the impact of the decrease in tropical and subtropical lower stratospheric ozone between experiment A (and, by definition C1/C2) and B (Fig. 3a), which mainly arises as a result of an accelerated Brewer-Dobson circulation (BDC, Supplementary Fig. S2), a ubiquitous feature in climate model projections under increased atmospheric CO₂ concentrations^{4,13}. The increase in middle and upper stratospheric ozone due to the slowing of catalytic ozone depletion cycles¹⁴ under CO₂-induced cooling¹⁵ of the stratosphere is also well understood. The local decrease in ozone induces a significant cooling of the lower and middle tropical stratosphere of up to 3.5°C in experiment B relative to C1 (Fig. 3b). An important feedback resulting from this decrease in tropical tropopause temperature is a relative drying of the stratosphere by ~4 ppmv in experiment B compared to C1/C2 (Supplementary Fig. S3). Since stratospheric water vapour is a greenhouse gas, this amplifies the tropospheric cooling due to the tropical and subtropical decreases in lower stratospheric ozone, and thus also contributes to changes in α (refs 16,17).

It is well-known that composition changes can modify the radiative balance of the atmosphere. However, our results demonstrate that the choice of how to include stratospheric composition feedbacks in climate models can be of first order importance for projections of global climate change. We diagnose radiative effects due to the differences in ozone and stratospheric water vapour between B and C1 of -0.68 Wm^{-2} and -0.78 Wm^{-2} , respectively (see also Methods and Supplementary Figure S4). The magnitude of this effect is related to the strong dependency of the LW radiative impact of ozone and stratospheric water vapour changes on their latitudinal and vertical structure. For instance, the low temperatures in the tropical upper troposphere and lower stratosphere (UTLS) make ozone changes in this region particularly important for the global energy budget^{18,19}. Consequently, climate models need to capture ozone changes here realistically; the tropical UTLS is a crucially sensitive region for climate models. However, trends in tropical tropopause height under climate change differ between models and depend on the forcing scenario²⁰. This suggests a potential mismatch between vertical temperature and prescribed ozone profiles in climate models which do not calculate ozone interactively. Such a mismatch would not only affect the direct radiative impact of ozone, but could also trigger inconsistent local heating or cooling in the cold trap region, which is crucial for the magnitude of the stratospheric water vapour feedback.

The magnitude of the overall feedback is expected to be strongly model-dependent, see for example the study by Dietmüller *et al.* (ref. 8) with a less well resolved stratosphere. The simulated BDC (and thus ozone) trends are closely related to the degree of tropospheric warming (ref. 21), which differs between models. The exact scaling of the ozone and water vapour response with tropospheric warming, in turn, will depend on other model-dependent factors, including the representation of gravity waves, the representation of the stratosphere, tropopause dehydration, lightning NO_x , other Earth system feedbacks, as well as the model base state²². Prescribing an ozone field which is neither consistent with the model nor with the forcing scenario, as in some CMIP5 experiments, will also lead to an inconsistent representation of the feedback. Consequently, further modelling studies are needed to investigate how such inter-model differences affect the magnitude of this feedback among a range of models.

The UTLS ozone changes are also key to understanding the differences in $\alpha_{\text{cre,lw}}$ (Fig. 2c). To isolate the dominant changes from 50°N to 50°S , we use regional Gregory regressions (Supplementary Fig. S5; ref. 23). We find a significant increase in UTLS cirrus clouds in this region in B compared with C1 (Fig. 4 and Supplementary Fig. S6), in agreement with the sensitivity of cirrus cloud formation to atmospheric temperature (Fig. 3b; ref. 24). This reduces the magnitude of the negative $\alpha_{\text{cre,lw}}$ in B compared to C1, consistent with the effects of high-altitude cirrus clouds on the LW energy budget²⁴⁻²⁶. More studies are needed to quantify how this effect could add to the large uncertainty in cloud feedbacks found in state-of-the-art climate models^{12,24-26}. However, we highlight the large range in the magnitude of $\alpha_{\text{cre,lw}}$ arising as a result of varying the treatment of ozone. This has obvious implications for studies in which cloud feedbacks are compared between models irrespective of their representation of stratospheric chemistry^{1,2,12}.

In conclusion, our results demonstrate the potential for considerable sensitivity of global warming projections to the representation of stratospheric composition feedbacks. We highlight the tropical UTLS as a key region for further study and emphasize the need for similar studies; including other climate feedbacks and their interactions in increasingly sophisticated Earth system models. Our results imply that model- and scenario-consistent representations of ozone are required, in contrast to the procedure applied widely in climate change assessments. These include quadruple CO₂ experiments, where changes in ozone are often not considered, as well as other CMIP5 and GeoMIP integrations where the majority of models specified inconsistent ozone changes. We note that further increasing model resolution will not address this fundamental issue. Consequently, we see a pressing need to invest more effort into producing model- and scenario-specific ozone datasets, or to move to a framework in which all participating models explicitly represent atmospheric chemical processes.

Methods

Model set-up

A version of the recently developed atmosphere-ocean coupled configuration of the Hadley Centre Global Environment Model version 3 (HadGEM3-AO) from the United Kingdom Met Office has been employed here⁹. It consists of three submodels, representing the atmosphere plus land surface, ocean and sea-ice.

For the atmosphere, the Met Office's Unified Model (MetUM) version 7.3 is used. The configuration used here is based on a regular grid with a horizontal resolution of 3.75° longitude by 2.5° latitude and comprises 60 vertical levels up to a height of ~84 km, and so includes a full representation of the stratosphere. Its dynamical core is non-hydrostatic and employs a semi-Lagrangian advection scheme. Subgrid-scale features such as clouds and gravity waves are parameterised.

The ocean component is the Nucleus for European Modelling of the Ocean (NEMO) model version 3.0 coupled to the Los Alamos sea ice model CICE version 4.0. It contains 31 vertical levels reaching down to a depth of 5 km. The NEMO configuration used in this study deploys a tripolar, locally anisotropic grid which has 2° resolution in longitude everywhere, but an increased latitudinal resolution in certain regions with up to 0.5° in the tropics.

Atmospheric chemistry is represented by the United Kingdom Chemistry and Aerosols (UKCA) model in an updated version of the detailed stratospheric chemistry configuration¹⁰ which is coupled to the MetUM. A simple tropospheric chemistry scheme is included which provides for emissions of 3 chemical species and constrains surface mixing ratios of 6 further species. This includes the surface mixing ratios of nitrous oxide (280 ppbv) and methane (790 ppbv), which effectively keeps their concentrations in the troposphere constant at approximately pre-industrial levels. Changes in photolysis rates in the troposphere and the stratosphere are calculated interactively using the Fast-JX photolysis scheme²⁷.

Linear climate feedback theory

The theory is based on the following equation described by Gregory *et al.*¹¹

$$N = F + \alpha \Delta T_{\text{surf}}$$

where N is the change in global mean net TOA radiative imbalance (Wm^{-2}), F the effective forcing (Wm^{-2}), T_{surf} the global-mean surface temperature change ($^{\circ}\text{C}$), and α the climate feedback parameter ($\text{W m}^{-2} \text{ } ^{\circ}\text{C}^{-1}$). Thus, α can be obtained by regressing N as a function of time against T_{surf} relative to a control climate. Here, the positive sign convention is used, meaning that a negative α implies a stable climate system. The theory assumes that the net climate feedback parameter can be approximated by a linear superposition of processes which contribute to the overall climate response to an imposed forcing. This can be expressed in form of a linear decomposition of the α parameter into process-related parameters

$$\alpha = \sum \lambda_i$$

with λ_i for example being $\lambda_{\text{water feedback}}$, λ_{clouds} etc. Similarly, one can decompose the climate feedback parameter into separate radiative components^{12,23,25}

$$\alpha = \alpha_{cs} + \alpha_{cre} = \alpha_{cs,sw} + \alpha_{cs,lw} + \alpha_{cre,sw} + \alpha_{cre,lw}$$

providing individual shortwave (SW) and longwave (LW) components for clear-sky (CS) radiative fluxes and the cloud radiative effect (CRE). In this method, the CRE contains direct cloud radiative effects and indirect cloud masking effects, e.g. due to persistent cloud cover which masks surface albedo changes in the all-sky calculation^{25,26}.

Radiative Transfer Experiments

The radiative transfer calculations were carried out using a version of the Edwards and Slingo²⁸ offline radiative transfer code updated to use the correlated-k method for calculating transmittances²⁹. This is identical to the radiation code used in the coupled model simulations. The inferred all-sky radiative effects due to the changes in ozone and stratospheric water vapour between experiments B and C1 were diagnosed using a base climatology (temperature, pressure, humidity etc.) taken from the last 50 years of C1 and perturbing around this state with the B minus C1 ozone or stratospheric water vapour fields over the same time period. The calculations employ the fixed dynamical heating (FDH) method¹⁵, in which stratospheric temperatures are adjusted to re-establish radiative equilibrium in the presence of the imposed perturbation (see ref. 30 for details). The radiative forcing is then diagnosed as the imbalance in the total (LW+SW) net (down minus up) tropopause fluxes. Note that the changes in ozone and stratospheric water vapour described in the study could be considered as a part forcing and part climate feedback. For example, the increase in ozone in the mid and upper stratosphere in Fig. 3a is linked to the CO_2 induced cooling at these levels, and may therefore not be strongly correlated with surface temperature change. In contrast, the decrease in ozone in the tropical mid- and

lower-stratosphere is driven by the strengthening in the Brewer-Dobson circulation, which is more closely linked to tropospheric temperature change²¹. However, for the purposes of quantifying the radiative contribution of the composition changes to the evolution of global climate in the experiments, we impose them diagnostically in the offline code as a pseudo radiative forcing agent.

Supplementary Material

Refer to Web version on PubMed Central for supplementary material.

Acknowledgements

We thank the European Research Council for funding through the ACCI project, project number 267760. The model development was part of the QUEST-ESM project supported by the UK Natural Environment Research Council (NERC) under contract numbers RH/H10/19 and R8/H12/124. We acknowledge use of the MONSooN system, a collaborative facility supplied under the Joint Weather and Climate Research Programme, which is a strategic partnership between the UK Met Office and NERC. A.C.M. acknowledges support from an AXA Postdoctoral Research Fellowship. For plotting, we used Matplotlib, a 2D graphics environment for the Python programming language developed by J. D. Hunter. We are grateful for advice of Paul Telford during the model development stage of this project and thank the UKCA team at the UK Met Office for help and support.

References

1. Taylor KE, Stouffer RJ, Meehl GA. An overview of CMIP5 and the experiment design. *Bull. Amer. Meteor. Soc.* 2012; 93:485–498.
2. Kravitz B, et al. An overview of the Geoengineering Model Intercomparison Project (GeoMIP). *J. Geophys. Res. Atmos.* 2013; 118:13103–13107.
3. Cionni I, et al. Ozone database in support of CMIP5 simulations: results and corresponding radiative forcing. *Atmos. Chem. Phys.* 2011; 11:11267–11292.
4. Eyring V, et al. Long-term ozone changes and associated climate impacts in CMIP5 simulations. *J. Geophys. Res. Atmos.* 2013; 118:5029–5060.
5. Jones CD, et al. The HadGEM2-ES implementation of CMIP5 centennial simulations. *Geosci. Model Dev.* 2011; 4:543–570.
6. Knutti R, Sedláček J. Robustness and uncertainties in the new CMIP5 climate model projections. *Nat. Clim. Change.* 2013; 3:369–373.
7. Son S-W, et al. The impact of stratospheric ozone recovery on the Southern Hemisphere westerly jet. *Science.* 2008; 320:1486–1489. [PubMed: 18556557]
8. Dietmüller S, Ponater M, Sausen R. Interactive ozone induces a negative feedback in CO₂-driven climate change simulations. *J. Geophys. Res. Atmos.* 2014; 119:1796–1805.
9. Hewitt HT, et al. Design and implementation of the infrastructure of HadGEM3: the next-generation Met Office climate modelling system. *Geosci. Model Dev.* 2011; 4:223–253.
10. Morgenstern O, et al. Evaluation of the new UKCA climate-composition model – Part 1: The stratosphere. *Geosci. Model Dev.* 2009; 2:43–57.
11. Gregory JM, et al. A new method for diagnosing radiative forcing and climate sensitivity. *Geophys. Res. Lett.* 2004; 31:L03205.
12. Andrews T, Gregory JM, Webb MJ, Taylor KE. Forcing, feedbacks and climate sensitivity in CMIP5 coupled atmosphere-ocean climate models. *Geophys. Res. Lett.* 2012; 39:L09712.
13. Meul S, Langematz U, Oberländer S, Garny H, Jöckel P. Chemical contribution to future tropical ozone change in the lower stratosphere. *Atmos. Chem. Phys.* 2014; 14:2959–2971.
14. Haigh JD, Pyle JA. Ozone perturbation experiments in a two-dimensional circulation model. *Q. J. Roy. Meteorol. Soc.* 1982; 108:551–574.
15. Fels SB, Mahlman JD, Schwarzkopf MD, Sinclair RW. Stratospheric sensitivity to perturbations in ozone and carbon dioxide: radiative and dynamical response. *J. Atmos. Sci.* 1980; 37:2265–2297.

16. Stuber N, Ponater M, Sausen R. Is the climate sensitivity to ozone perturbations enhanced by stratospheric water vapor feedback? *Geophys. Res. Lett.* 2001; 28:2887–2890.
17. Stuber N, Ponater M, Sausen R. Why radiative forcing might fail as a predictor of climate change. *Clim. Dyn.* 2005; 24:497–510.
18. Lacis AA, Wuebbles DJ, Logan JA. Radiative forcing of climate by changes in the vertical distribution of ozone. *J. Geophys. Res. Atmos.* 1990; 95:9971–9981.
19. Hansen J, Sato M, Ruedy R. Radiative forcing and climate response. *J. Geophys. Res. Atmos.* 1997; 102:6831–6864.
20. Santer BD, et al. Contributions of anthropogenic and natural forcing to recent tropopause height changes. *Science.* 2003; 301:479–483. [PubMed: 12881562]
21. Shepherd TG, McLandress C. A robust mechanism for strengthening of the Brewer-Dobson circulation in response to climate change: critical-layer control of subtropical wave breaking. *J. Atmos. Sci.* 2011; 68:784–797.
22. Hsu J, Prather MJ, Bergmann D, Cameron-Smith P. Sensitivity of stratospheric dynamics to uncertainty in O₃ production. *J. Geophys. Res. Atmos.* 2013; 118:8984–8999.
23. Boer GJ, Yu B. Climate sensitivity and response. *Clim. Dyn.* 2003; 20:415–429.
24. Kuebbeler M, Lohmann U, Feichter J. Effects of stratospheric sulfate aerosol geo-engineering on cirrus clouds. *Geophys. Res. Lett.* 2012; 39:L23803.
25. Webb MJ, et al. On the contribution of local feedback mechanisms to the range of climate sensitivity in two GCM ensembles. *Clim. Dyn.* 2006; 27:17–38.
26. Zelinka MD, et al. Contributions of different cloud types to feedbacks and rapid adjustments in CMIP5. *J. Clim.* 2013; 26:5007–5027.
27. Telford PJ, et al. Implementation of the Fast-JX Photolysis scheme (v6.4) into the UKCA component of the MetUM chemistry-climate model (v7.3). *Geosci. Model Dev.* 2013; 6:161–177.
28. Edwards JM, Slingo A. Studies with a flexible new radiation code. I: Choosing a configuration for a large-scale model. *Q. J. Roy. Meteorol. Soc.* 1996; 122:689–719.
29. Cusack S, Edwards JM, Crowther JM. Investigating k distribution methods for parameterizing gaseous absorption in the Hadley Centre Climate Model. *J. Geophys. Res. Atmos.* 1999; 104:2051–2057.
30. Maycock AC, Shine KP, Joshi MM. The temperature response to stratospheric water vapour changes. *Q. J. Roy. Meteorol. Soc.* 2011; 137:1070–1082.

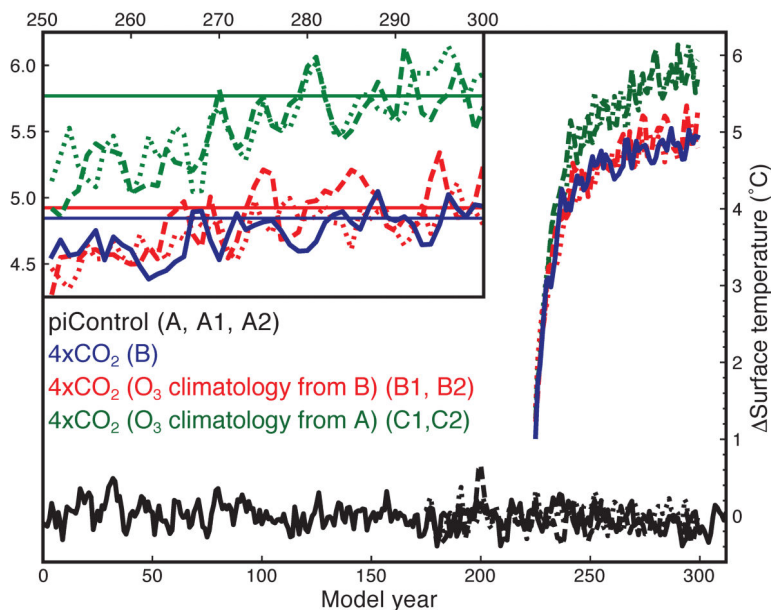


Figure 1. Temporal evolution of the annual and global mean surface temperature anomalies
 All anomalies (°C) are shown relative to the average temperature of experiment A. Solid lines show the interactive chemistry runs (A, B), dashed lines the 3D climatology experiments (A1, B1, C1) and dotted lines the 2D climatology experiments (A2, B2, C2). For clarity, lines for the abrupt4×CO₂ experiments start after year one so that they are not joined with those of the corresponding control experiments. The last 50 years of the abrupt4×CO₂ experiments are highlighted in the inset panel with the straight lines marking the average temperature in each set of experiments over the last 20 years.

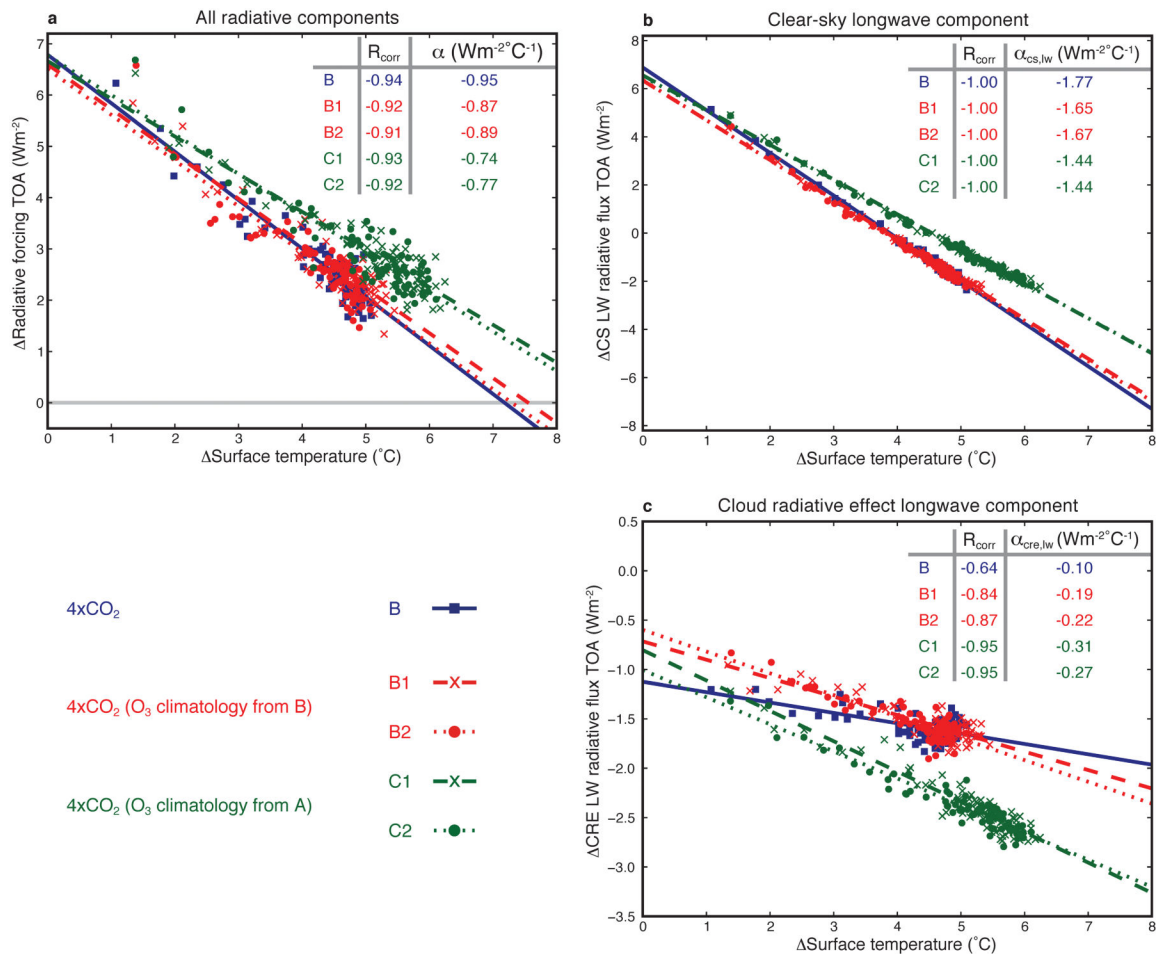


Figure 2. Gregory regression plots

a, For all radiative components, giving an ~25% larger climate feedback parameter, α , in C1/C2 than in B. **b, c**, For the CS-LW and CRE-LW components only. In particular in **c**, a clear evolution of the atmospheric state B is observable as it starts off very close to C1 and C2 and evolves towards B1 and B2. Radiative fluxes follow the downward sign convention so that all negative (positive) changes in α imply a cooling (warming) effect. The inset tables give the correlation coefficient (R_{corr}) and the α parameter obtained from each regression.

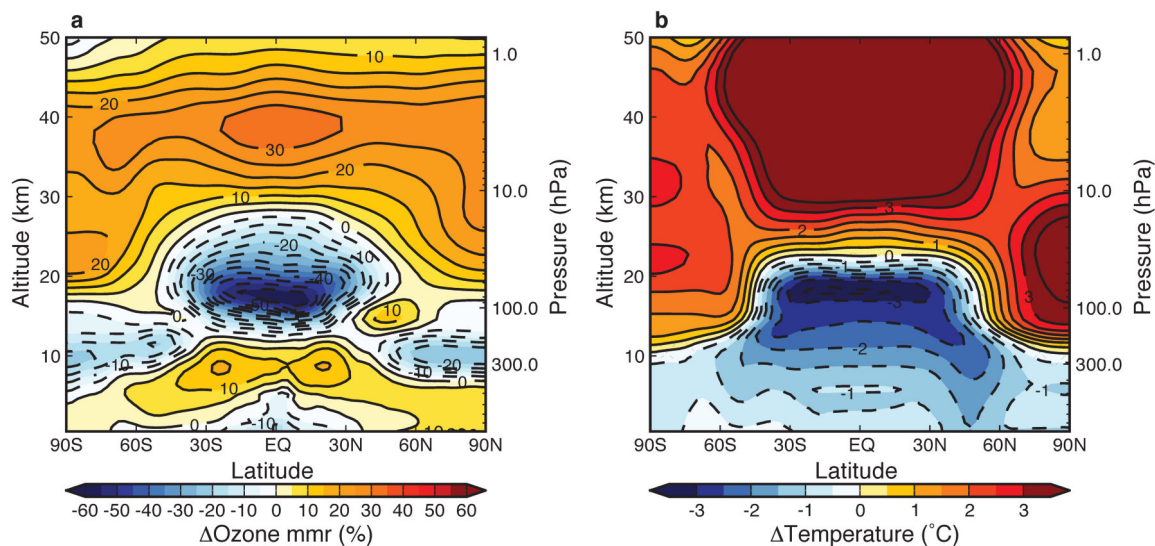


Figure 3. Annual and zonal mean differences in ozone and temperature

Shown are averages over the last 50 years of each experiment. **a**, The percentage differences in ozone between simulations B and A. By definition, these are identical to the differences in the climatologies between B/B1/B2 and C1/C2/A/A1/A2. Note that the climatologies of experiments B1/B2 and other 2D and 3D versions of each set of experiment are only identical after zonal averaging. **b**, The absolute temperature anomaly ($^{\circ}\text{C}$) between experiments B and C1. Apart from some areas around the tropopause (hatched out), all differences in **b** are statistically significant at the 95% confidence level using a two-tailed Student's t-test.

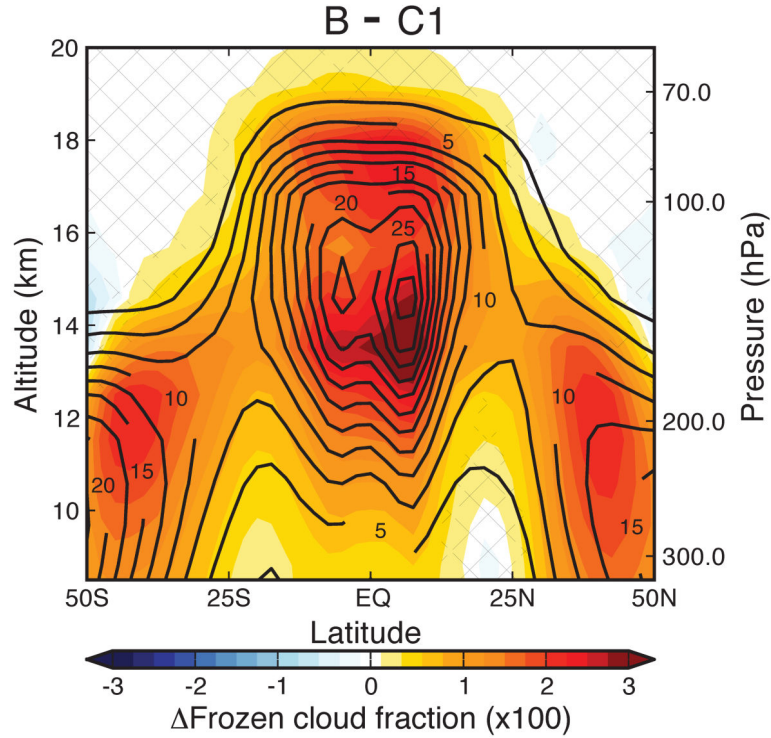


Figure 4. Cirrus cloud changes

Zonal and annual mean frozen cloud fraction per unit volume multiplied by factor 100 in the region 50°N-50°S where the deviations in $\alpha_{\text{cre,lw}}$ are found. The shading shows the difference B minus C1 averaged over the last 50 years of both experiments. Contour lines (interval 2.5) denote the climatology of C1. Note that the tropical cloud fraction increases at ~12-13 km mainly result from the relatively warmer climate in C1. They therefore do not change $\alpha_{\text{cre,lw}}$, in contrast to the increases in the UTLS, see also Figure S6. Non-significant differences (using a two-tailed Student's t-test at the 95% confidence level or where the cloud fraction in both experiments is smaller than 5‰) are hatched out.

Table 1
Overview of the experiments

Experiment	Description	Initial Condition	Chemistry
A	piControl, (285 ppmv CO ₂)	Initialised from 900 year spin-up	Interactive
A1	piControl-1, (285 ppmv CO ₂)	Initialised from A (year 175)	Non-interactive, 3D climatologies from A
A2	piControl-2, (285 ppmv CO ₂)	Initialised from A (year 175)	Non-interactive, 2D climatologies from A
B	abrupt4×CO ₂ (1140 ppmv CO ₂)	Initialised from A (year 225)	Interactive
B1	abrupt4×CO ₂ (1140 ppmv CO ₂)	Initialised from A1 (year 50)	Non-interactive, 3D climatologies from B
B2	abrupt4×CO ₂ (1140 ppmv CO ₂)	Initialised from A2 (year 50)	Non-interactive, 2D climatologies from B
C1	abrupt4×CO ₂ (1140 ppmv CO ₂)	Initialised from A1 (year 50)	Non-interactive, 3D climatologies from A
C2	abrupt4×CO ₂ (1140 ppmv CO ₂)	Initialised from A2 (year 50)	Non-interactive, 2D climatologies from A

Climatologies for the non-interactive runs represent the seasonal cycle on a monthly-mean basis. 3D climatologies contain chemical fields of the most important radiatively active species (ozone, methane, and nitrous oxide) for all spatial dimensions (longitude, latitude, altitude). For 2D climatologies these fields were averaged over all longitudes, as it is commonly done for ozone climatologies used in non-interactive climate integrations^{3,5}.